Table 3. *The size of the reaction cavity and reaction rate for some cobaloxime complexes*

	V (Å^3)	Reaction rate ($\times 10^{-6}$ s^{-1})
R-depp	8.40	–*
R-dpep	10.18	–
R-tbp	10.64	–
R-tpp	11.31	–
R-pyrr	11.55	1.69
S-*S*-pea	12.23	2.38
R-*S*-pea	14.53	3.13
R-dmpp	17.97	4.80†

* Racemization was not observed at room temperature.
† Value determined from the site occupancy of ce group.

temperature. This table clearly indicates that the larger the reaction cavity is, the greater the reaction rate. A volume greater than 11.5 Å^3 appears necessary for racemization.

The above results suggest that the reactivity of the ce group depends on the size of the cavity and that the hydrogen bond may play no role in the racemization. In the β–α solid-state photoisomerization, the β-ce group bonded to the cobalt atom was changed to an α-ce group. If the N atom of the β-ce group was connected by a hydrogen bond with the solvent molecule, the isomerization rate became faster. It was proposed that the hydrogen bond would stabilize the β-ce radical produced by the Co—C bond cleavage and that it may accelerate the β–α radical transformation (Sekine & Ohashi, 1991). In the racemization, on the other hand, the α-ce radical, produced by the Co—C bond breaking, may be stable and may not be affected by the hydrogen bond. Therefore, the reaction rate depends only on the size of the cavity for the ce group.

This work was partly supported by a Grant-in-Aid for Scientific Research from the Ministry of Education, Science and Culture, Japan.

References

Kojima, Y., Iwasaki, S., Ohashi, Y., Baba, S. & Ohgo, Y. (1991). *Acta Cryst.* **C47**, 300–303.

Kurihara, T., Uchida, A., Ohashi, Y., Sasada, Y., Ohgo, Y. & Baba, S. (1983). *Acta Cryst.* **B39**, 431–437.

Main, P., Hull, S. E., Lessinger, L., Germain, G., Declercq, J.-P. & Woolfson, M. M. (1978). *MULTAN78. A System of Computer Programs for the Automatic Solution of Crystal Structures from X-ray Diffraction Data.* Univs. of York, England, and Louvain, Belgium.

Ohashi, Y. (1988). *Acc. Chem. Res.* **21**, 268–274.

Ohashi, Y., Sasada, Y. & Ohgo, Y. (1978). *Chem. Lett.* pp. 743–746.

Ohashi, Y., Uchida, A., Sasada, Y. & Ohgo, Y. (1983). *Acta Cryst.* **B39**, 54–61.

Ohashi, Y., Yanagi, K., Kurihara, T., Sasada, Y. & Ohgo, Y. (1981). *J. Am. Chem. Soc.* **103**, 5805–5812.

Ohgo, Y., Takeuchi, S., Natori, Y., Yoshimura, J., Ohashi, Y. & Sasada, Y. (1981). *Bull. Chem. Soc. Jpn*, **54**, 3095–3099.

Sekine, A. & Ohashi, Y. (1991). *Bull. Chem. Soc. Jpn*, **64**, 2183–2187.

Sheldrick, G. M. (1976). *SHELX76*. Program for crystal structure determination. Univ. of Cambridge, England.

Tomotake, Y., Uchida, A., Ohashi, Y., Sasada, Y., Ohgo, Y. & Baba, S. (1984). *Acta Cryst.* **C40**, 1684–1687.

Tomotake, Y., Uchida, A., Ohashi, Y., Sasada, Y., Ohgo, Y. & Baba, S. (1985). *Isr. J. Chem.* **25**, 327–333.

Acta Cryst. (1993). **B49**, 277–282

Structure of Bis(2-amino-5-nitropyridinium) Dichromate as a Step Towards the Design of Efficient Organic–Inorganic Non-Linear Optical Crystals

By J. Pecaut and R. Masse

*Laboratoire de Cristallographie associé à l'Université Joseph Fourier, CNRS, BP 166,
38042 Grenoble CEDEX 09, France*

(*Received* 4 *February* 1992; *accepted* 10 *August* 1992)

Abstract

The orthorhombic crystal structure of $2C_5H_6N_3O_2^+.Cr_2O_7^{2-}$ [$a = 22.454$ (6), $b = 15.129$ (2), $c = 5.189$ (2) Å, $Z = 4$, orthorhombic, $P2_1nb$, $D_x = 1.866$ g cm^{-3}] has been solved using direct methods and refined to $wR = 0.029$ for 2514 reflections. This study provides a step towards a new route to obtain non-linear optical crystals which aims at combining the highly polarizable 2-amino-5-nitropyridinium cation with inorganic anionic host matrices. The shielding effect of dichromate anions in the building of an acentric polar framework is discussed. The structure is compared with other structures containing 2-amino-5-nitropyridine moieties. The cations are completely or partly arranged in a 'herringbone' structure in all these frameworks.

Introduction

Research into very effcient and highly transparent non-linear optical crystals (range: 100 nm to IR

0108-7681/93/020277-06$06.00

Table 1. *Progressive structural approach towards the design of 2-amino-5-nitropyridinium dihydrogenmonophosphate, a highly efficient organic–inorganic non-linear optical crystal*

	$(NO_3)^-$	$(CuCl_4)^{2-}$	$(COO^-)_2$	$(Cr_2O_7)^{2-}$	$(SO_4)^{2-}$	$(HSO_4^-)_n$	$(H_2PO_4^-)_n$	$(C_4H_5O_6^-)_n$
SHG powder test	–	–	–	+	–	–	+	–
Crystal symmetry	$P2_1/n$	$P2_1/c$		$P2_1nb$		$Pcab$	$Pna2_1$	$P2_1$
Structure solved	Yes	Yes	No	Yes	No	Yes	Yes	Yes
Situation of 2A5NP⁺ cations	Antiparallel ordering	One site has polar ordering		Polar packing with pseudo-inversion centres		Antiparallel ordering	Polar packing	Polar packing
Average volume of anionic unit (Å^3)	50	147		150	80	80	85	140
References	(*a*)	(*a*)		(*b*)		(*c*)	(*d*)	(*e*)

References: (*a*) Bagieu-Beucher, Masse & Tranqui (1991), (*b*) this work, (*c*) Pecaut, Le Fur & Masse (1992), (*d*) Masse & Zyss (1991), (*e*) Masse, Zyss, Bagieu-Beucher & Levy (1993).

wavelengths) is a challenge in which physicists concerned with non-linear optics are today engaged. The performance of optical signal-processing devices is linked to the discovery of such new materials (Zyss, 1990). A large variety of organic and inorganic non-linear optical crystals have been proposed during the past 20 years. Most noteworthy are the organic crystals: 3-methyl-4-nitropyridine 1-oxide (Zyss, Chemla & Nicoud, 1981), *N*-4-nitrophenyl-L-prolinol (Zyss, Nicoud & Coquillay, 1984), 3-methyl-4-methoxy-4′-nitrostilbene (Tam, Guerin, Calabrese & Stevenson, 1989); and the inorganic crystals: $Ba_3(B_3O_6)_2$ (Lu, Ho & Huang, 1982; Chen, Wu, Jiang & You, 1984), LiB_3O_5 (Chen, Wu, Jiang, Wu, Li & Lin, 1989), $KTiOPO_4$ (Zumsteg, Bierlein & Gier, 1976; Bierlein & Vanherzeele, 1989). The most efficient crystalline organic materials exhibit large quadratic susceptibilities associated with a target transparency limit of 500 nm in contrast to the inorganic materials where weaker quadratic susceptibilities are combined with a large transparency range ($\lambda_{\text{cut-off}} = 160$ nm for LiB_3O_5). Therefore, two crystal-engineering routes may be suggested with a view to obtaining an optimal transparency efficiency trade-off.

In inorganic materials built up by $B_3O_6^{3-}$ trimetaborate anions (BBO) or $(TiO_6)_n$ polymeric chains (KTP), the densification of associated oscillators could be achieved by changing the cationic matrices, the major difficulty being how to induce acentric packing.

In organic materials, the building of acentric packings is less problematic, and the specific ionization of charge-transfer molecules like nitroanilines and stilbenes shifts the crystal absorption boundary towards blue wavelengths because of the inherently less polarizable nature of such ions (Dewar, 1950). This strategy has been already proposed by Meredith (1983) in stilbene organic salts. The ionization involves the encapsulation of organic entities in organic or inorganic anionic host subnetworks. The selection of the anionic entity is crucial because it may or may not induce the final acentric packing. Applying this second approach, we have selected a nitroaniline derivative, 2-amino-5-nitropyridine, the charge-transfer character of which is not cancelled out by the ionization of pyridine ring. The encapsulation of 2-amino-5-nitropyridinium cations in various inorganic anionic host subnetworks (Table 1) demonstrates that the role of the counter-anion is important in obtaining crystal acentricity and the optimal packing of cations that induces large macroscopic quadratic non-linearities (Zyss & Oudar, 1982).

The aim of this work is to combine 2-amino-5-nitropyridinium cations with large dichromate anions ($V = 150$ Å^3) in the expectation of producing a cationic polar arrangement due to the possible shielding effect of the anionic subnetwork.

Experimental

Chemical preparation

0.002 mol of 2-amino-5-nitropyridine was dissolved in 20 cm^3 of pure acetic acid at 333 K. 2 cm^3 solution containing 0.002 mol CrO_3 was added. Slow evaporation, at room temperature, yielded prismatic crystals up to 0.20 × 0.30 × 0.55 mm in size. The pH had no influence on crystallization. Under these drastic conditions fibrous crystals or needles were easily obtained. Crystals were washed in methyl acetate. The chemical formula is based on the X-ray crystal structure determination.

Data-collection parameters

For data collection, a triangular based prismatic single crystal, 0.25 × 0.30 × 0.61 mm, was used. Orthorhombic unit-cell parameters were refined by least-squares methods using the angular data of 20 reflections ($10 < \theta < 12°$) measured with a four-circle diffractometer: $a = 22.454\,(6)$, $b = 15.129\,(2)$, $c = 5.189\,(2)$ Å, $V = 1762.9\,(8)$ Å^3, $Z = 4$, space group $P2_1nb$, $D_x = 1.866$ g cm^{-3}, $F(000) = 1000$. Data-collection details: Enraf–Nonius CAD-4 diffractometer, graphite monochromator, $\lambda(\text{Ag}\,K\bar{\alpha}) = 0.55941$ Å, $\mu = 6.589$ cm^{-1}, ω scan, scan width = 1.20°, scan speed between 0.027 and 0.119° s^{-1}; total reflection measuring time 10.9–44 s; 5937 reflections measured between 2 and 30° θ, 2545 conserved, satisfying the condition $I_o > 3\sigma(I_o)$; $h_{\min} = 1$, $k_{\min} = l_{\min} = 0$, $h_{\max} = 40$, $k_{\max} = 27$, $l_{\max} = 9$. Intensity reference reflections $\overline{16},2,0$ and $\overline{11},1,2$ showed no significant variation. Lorentz and polarization corrections were applied. No absorption correction. Secondary-extinction correction: $g = 10^{-6}$ (Stout & Jensen, 1968). The structure was solved by direct methods using *MULTAN* (Main, Lessinger, Woolfson, Germain & Declercq, 1977). Hydrogen atoms were located by difference Fourier syntheses. Anisotropic full-matrix least-squares refinements were performed on F, using the following weighting scheme: $w = 1/\sigma^2(F_o) = 4F_o^2/[\sigma^2(I_o) + (pF_o^2)^2]$; $p = 0.01$. Hydrogen atoms were refined isotropically. Final refinement with 2514 independent reflections: no reflections rejected. Final $R = 0.027$, $wR = 0.029$, $S = 1.74$. Maximum shift/e.s.d. = 0.14. Maximum and minimum peak heights in the final difference Fourier map were $+0.73$ and -0.40 e Å^{-3}. Scattering factors for neutral atoms and f', f'' were taken from *International Tables for X-ray Crystallography* (1974, Vol. IV). The Enraf–Nonius *Structure Determination Package* (Enraf–Nonius, 1977) was used for all calculations with a MicroVAXII computer. The structure was drawn using the *ORTEP* program (Johnson, 1965). Table 2 lists atomic coordinates and thermal parameters.*

Table 2. *Atomic positions and* B_{eq} *values* (Å^2) *with e.s.d.'s in parentheses*

$B_{eq} = (4/3)\sum_i\sum_j \beta_{ij}\mathbf{a}_i.\mathbf{a}_j$.

	x	y	z	B_{eq}, B_{iso}* (Å^2)
Cr(1)	0.000	0.31595 (2)	0.75666 (7)	2.064 (5)
Cr(2)	−0.04770 (2)	0.51297 (3)	0.73989 (7)	2.321 (5)
O(1)	0.00653 (9)	0.4312 (1)	0.8389 (4)	2.69 (3)
O(2)	0.05992 (9)	0.2707 (1)	0.8782 (4)	3.09 (4)
O(3)	−0.00004 (1)	0.3056 (1)	0.4505 (3)	3.16 (4)
O(4)	−0.06024 (9)	0.2787 (1)	0.8803 (4)	3.34 (4)
O(5)	−0.10956 (9)	0.4995 (2)	0.8889 (4)	3.49 (4)
O(6)	−0.0166 (1)	0.6059 (1)	0.8189 (4)	3.85 (5)
O(7)	−0.0557 (1)	0.5072 (2)	0.4342 (4)	3.86 (4)
N(1)	0.0576 (1)	0.1303 (2)	0.2433 (5)	3.67 (5)
N(2)	0.0803 (1)	−0.0184 (2)	0.2641 (4)	2.59 (4)
N(3)	0.1738 (1)	−0.1661 (2)	−0.1194 (6)	4.65 (6)
C(1)	0.0861 (1)	0.0616 (2)	0.1476 (5)	2.56 (4)
C(2)	0.1232 (1)	0.0673 (2)	−0.0730 (6)	3.23 (5)
C(3)	0.1090 (1)	−0.0922 (2)	0.1812 (5)	2.67 (5)
C(4)	0.1444 (1)	−0.0857 (2)	−0.0297 (6)	3.01 (5)
C(5)	0.1516 (1)	−0.0061 (2)	−0.1595 (6)	3.45 (6)
O(8)	0.1703 (1)	−0.2324 (2)	0.0118 (6)	5.89 (6)
O(9)	0.1997 (1)	−0.1608 (3)	−0.3269 (6)	7.51 (8)
H(1)	0.035	0.125	0.347	2.0*
H(2)	0.064	0.179	0.146	1.2*
H(3)	0.058	−0.030	0.370	3.4*
H(4)	0.103	−0.148	0.280	1.1*
H(5)	0.183	0.002	−0.331	3.3*
H(6)	0.128	0.122	−0.162	1.0*
N(4)	0.3860 (1)	0.3343 (2)	−0.2159 (5)	4.08 (6)
N(5)	0.3646 (1)	0.1862 (2)	−0.2166 (4)	2.56 (4)
N(6)	0.2726 (1)	0.0395 (2)	0.1689 (6)	4.37 (6)
C(6)	0.3573 (1)	0.2673 (2)	−0.1112 (6)	2.75 (5)
C(7)	0.3177 (2)	0.2745 (2)	0.0980 (6)	3.47 (6)
C(8)	0 2895 (1)	0.2011 (3)	0.1896 (6)	3.52 (6)
C(9)	0.3002 (1)	0.1197 (2)	0.0720 (6)	2.88 (5)
C(10)	0.3379 (1)	0.1128 (2)	−0.1304 (6)	2.77 (5)
O(10)	0.2791 (1)	−0.0291 (2)	0.0504 (6)	5.22 (6)
O(11)	0.2438 (2)	0.0461 (2)	0.3675 (6)	7.23 (7)
H(7)	0.415	0.323	−0.332	3.4*
H(8)	0.387	0.387	−0.118	3.0*
H(9)	0.308	0.335	0.170	1.6
H(10)	0.263	0.207	0.320	1.2*
H(11)	0.348	0.058	−0.212	1.0*
H(12)	0.384	0.183	−0.327	1.5*

Symmetry code in $P2_1nb$: x, y, z; $\frac{1}{2}+x, -y, -z$; $\frac{1}{2}+x, \frac{1}{2}-y, \frac{1}{2}+z$; $x, \frac{1}{2}+y, \frac{1}{2}-z$.

Discussion

The dichromate anions are stacked along the **b** axis, associated in chains located at the positions $\frac{1}{2}\mathbf{a}$, $\frac{1}{4}\mathbf{c}$ and $\mathbf{a}$, $\frac{3}{4}\mathbf{c}$. The 2-amino-5-nitropyridinium (2A5NP$^+$) cations are anchored onto these chains through hydrogen bonds so that a double polar cationic layer is built up. The most interesting feature is shown in Figs. 1 and 2, in which the acentric anionic subnetwork is compared with the pseudo-centric packing of polar cations. The role of large dichromate anions is to induce a shielding effect which precludes the dipole–dipole interactions inherent in 2-amino-5-nitropyridine entities. The geometrical features of 2A5NP$^+$ cations (Table 3) are close to those already observed in various 2-amino-5-nitropyridinium salts (referenced in Table 1): all conjugated bond lengths are shortened except the C—NO$_2$ terminal bond which is lengthened compared to the *p*-nitroaniline C—N and C—C bonds [C—NO$_2$ = 1.460 (5) and 1.453 (4) Å *versus* 1.434 (2) Å in *p*-nitroaniline] (Trueblood, Goldish & Donohue, 1961; Colapietro, Domenicano, Marciante & Portalone, 1982). This situation, which is due to protonation of pyridine group, results in a shift of the transparency threshold towards blue wavelengths in crystals containing 2A5NP$^+$ cations compared to the yellow molecular crystals of 2-amino-5-nitropyridine (Dewar, 1950): the intramolecular charge transfer and the dipolar moment are not cancelled out. The protonation not only allows strong anchorage of 2A5NP$^+$ onto inorganic entities but also induces the formation of a second acceptor group NH$^+$ grafted onto the pyridine ring which competes with the electron-withdrawing NO$_2$ group. This is clearly shown by the contraction of C—C and C—NH$_2$ bonds in the pyridine ring (Table 3) with respect to the conjugated bond lengths of *p*-nitroaniline.

Unfortunately, pseudo-inversion centres are present between two independent cation sites. This observation is in good agreement with the weak second harmonic signal (Kurtz & Perry, 1968) resulting from the illumination of a powder sample by a

---

* Lists of structure factors, anisotropic thermal parameters, least-squares planes, and bond lengths and angles have been deposited with the British Library Document Supply Centre as Supplementary Publication No. SUP 55599 (20 pp.). Copies may be obtained through The Technical Editor, International Union of Crystallography, 5 Abbey Square, Chester CH1 2HU, England. [CIF reference: PA0281]

YAG:Nd^{3+} fundamental beam (1.06 μm). The pseudo-inversion centres appear in a region where the dichromate anions are separated by a minimum distance of 2.977 (3) Å. The sum of the van der Waals radii of the oxygen atoms is 3 Å if computed from Bondi's values (Bondi, 1964).

The hydrogen-bond scheme given in Table 3 reveals that the anchorage of both $2A5NP^+$ cations is made through one short and two long hydrogen bonds balancing the negative charges of the dichromate anions. O(7) and O(3) are not involved in the hydrogen-bond pattern. The shortest distance between $2A5NP^+$ cations [O(9)—O(10) = 3.315 (4) Å] corresponds to the minimum mutual repulsion of two neighbouring NO_2 goups in contrast to its equivalent for dichromate anions [O(4)—O(6) = 2.977 (3) Å].

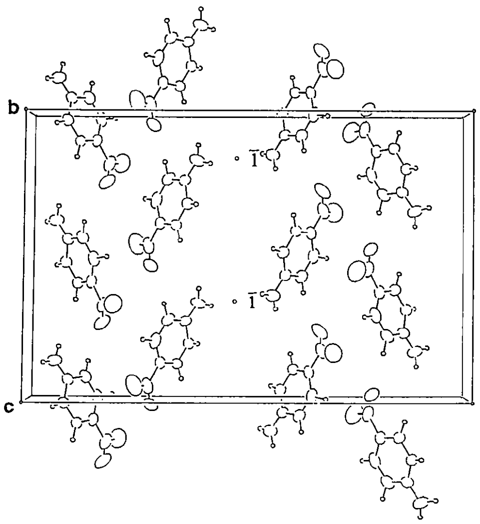

Fig. 1. Pseudo-centric packing of $2A5NP^+$ cations in bis(2-amino-5-nitropyridinium) dichromate.

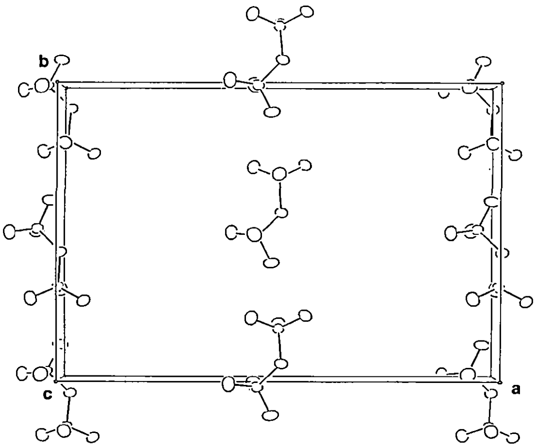

Fig. 2. Acentric arrangement of dichromate anions in bis(2-amino-5-nitropyridinum) dichromate.

Table 3. *Interatomic distances* (Å), *bond angles* (°) *and hydrogen-bonding geometry* (Å, °) *with e.s.d.'s in parentheses*

Dichromate anion			
Cr(1)—O(1)	1.801 (2)	O(1)—Cr(1)—O(2)	104.3 (1)
Cr(1)—O(2)	1.636 (2)	O(1)—Cr(1)—O(3)	109.4 (1)
Cr(1)—O(3)	1.597 (2)	O(1)—Cr(1)—O(4)	108.3 (3)
Cr(1)—O(4)	1.597 (2)	O(2)—Cr(1)—O(3)	110.3 (1)
Cr(2)—O(1)	1.810 (2)	O(2)—Cr(1)—O(4)	113.2 (1)
Cr(2)—O(5)	1.603 (2)	O(3)—Cr(1)—O(4)	111.1 (1)
Cr(2)—O(6)	1.622 (2)	O(1)—Cr(2)—O(5)	111.1 (1)
Cr(2)—O(7)	1.599 (2)	O(1)—Cr(2)—O(6)	103.4 (1)
		O(1)—Cr(2)—O(7)	108.7 (1)
		O(5)—Cr(2)—O(6)	111.2 (1)
O(4)—O(6)	2.977 (3)	O(5)—Cr(2)—O(7)	112.0 (1)
Cr(1)—Cr(2)	3.1686 (5)	O(6)—Cr(2)—O(7)	110.3 (1)
		Cr(1)—O(1)—Cr(2)	122.7 (1)
First 2-amino-5-nitropyridinium cation			
N(1)—C(1)	1.318 (4)	C(1)—N(1)—H(1)	121 (3)
N(1)—H(1)	0.75 (3)	C(1)—N(1)—H(2)	111 (2)
N(1)—H(2)	0.91 (3)	H(1)—N(1)—H(2)	127 (3)
N(2)—C(1)	1.360 (4)	C(2)—N(2)—C(3)	123.0 (2)
N(2)—C(3)	1.360 (4)	C(1)—N(2)—H(3)	126 (3)
N(2)—H(3)	0.76 (4)	C(3)—N(2)—H(3)	110 (3)
N(3)—C(4)	1.460 (5)	C(4)—N(3)—O(8)	118.6 (3)
N(3)—O(8)	1.215 (5)	C(4)—N(3)—O(9)	116.1 (3)
N(3)—O(9)	1.225 (5)	O(8)—N(3)—O(9)	125.2 (4)
C(1)—C(2)	1.419 (4)	N(1)—C(1)—N(2)	119.2 (3)
C(2)—C(5)	1.357 (5)	N(1)—C(1)—C(2)	122.8 (3)
C(2)—H(6)	0.95 (3)	N(2)—C(1)—C(2)	118.0 (3)
C(3)—C(4)	1.356 (4)	C(1)—C(2)—C(5)	119.5 (3)
C(3)—H(4)	1.00 (3)	C(1)—C(2)—H(6)	121 (2)
C(4)—C(5)	1.390 (5)	C(5)—C(2)—H(6)	120 (2)
C(5)—H(5)	1.15 (4)	N(2)—C(3)—C(4)	118.3 (3)
		N(2)—C(3)—H(4)	118 (2)
		C(4)—C(3)—H(4)	124 (2)
		N(3)—C(4)—C(3)	117.5 (3)
		N(3)—C(4)—C(5)	121.0 (3)
		C(3)—C(4)—C(5)	121.5 (3)
		C(2)—C(5) C(4)	119.7 (3)
		C(2)—C(5)—H(5)	118 (3)
		C(4)—C(5)—H(5)	123 (2)
Second 2-amino-5-nitropyridinium cation			
N(4)—C(6)	1.317 (4)	C(6)—N(4)—H(7)	118 (3)
N(4)—H(7)	0.91 (4)	C(6)—N(4)—H(8)	116 (2)
N(4)—H(8)	0.95 (4)	H(7)—N(4)—H(8)	120 (4)
N(5)—C(6)	1.353 (4)	C(6)—N(5)—C(10)	124.2 (2)
N(5)—C(10)	1.341 (4)	C(6)—N(5)—H(12)	117 (3)
N(5)—H(12)	0.72 (3)	C(10)—N(5)—H(12)	117 (3)
N(6)—C(9)	1.453 (4)	C(9)—N(6)—O(10)	119.1 (3)
N(6)—O(10)	1.215 (4)	C(9)—N(6)—O(11)	116.8 (3)
N(6)—O(11)	1.220 (4)	O(10)—N(6)—O(11)	124.1 (3)
C(6)—C(7)	1.408 (4)	N(4)—C(6)—N(5)	118.1 (3)
C(7)—C(8)	1.363 (5)	N(4)—C(6)—C(7)	124.6 (3)
C(7)—H(9)	1.01 (3)	N(5)—C(6)—C(7)	117.3 (3)
C(8)—C(9)	1.395 (5)	C(6)—C(7)—C(8)	120.0 (3)
C(8)—H(10)	0.90 (3)	C(6)—C(7)—H(9)	119 (2)
C(9)—C(10)	1.352 (4)	C(8)—C(7)—H(9)	121 (2)
C(10)—H(11)	0.96 (4)	C(7)—C(8)—C(9)	119.1 (3)
		C(7)—C(8)—H(10)	119 (2)
		C(9)—C(8)—H(10)	122 (2)
O(9)—O(10)	3.315 (4)	N(6)—C(9)—C(8)	120.8 (3)
		N(6)—C(9)—C(10)	118.1 (3)
		C(8)—C(9)—C(10)	121.1 (3)
		N(5)—C(10)—C(9)	118.4 (3)
		N(5)—C(10)—H(11)	117 (2)
		C(9)—C(10)—H(11)	124 (2)

Hydrogen bonding

	$d_{D—\mathrm{H}}$	$d_{\mathrm{H}—A}$	$d_{D—A}$	$\angle D$—H—A
N(1)—H(1)···O(6)	0.75 (3)	2.10 (3)	2.841 (4)	170 (4)
N(1)—H(2)···O(2)	0.91 (3)	1.96 (3)	2.848 (3)	163 (3)
N(2)—H(3)···O(1)	0.76 (4)	1.99 (4)	2.751 (3)	174 (5)
N(4)—H(7)···O(4)	0.91 (4)	2.21 (4)	2.962 (4)	140 (4)
N(4)—H(8)···O(5)	0.95 (4)	2.09 (4)	3.035 (4)	177 (3)
N(5)—H(12)···O(4)	0.72 (3)	2.05 (3)	2.739 (3)	160 (4)

The dichromate anionic framework provides a backbone onto which the cations are anchored in a polar ordering, but the introduction of local inversion centres cannot be inferred. The dimension of the dichromate anion is sufficient to act as a shield between the cations, but its charge is balanced using two cation sites: their densification can induce local dipole–dipole interactions which are responsible for the pseudo-centrosymmetry. An acceptable charge-dimension compromise of the anions which can host the $2A5NP^+$ cations in an acentric and non-linear optical efficient structure (Table 1) has been found using an $(H_2PO_4^-)_n$ polymeric counter-anion, an example being the 2-amino-5-nitropyridinium dihydrogenmonophosphate salt (Masse & Zyss, 1991).

Concluding remarks

A detailed and comparative inspection of the crystal structures of 2-amino-5-nitropyridinium salts illustrated in Figs. 3, 4, 5 and 6 reveals the role of anionic steric hindrance and charge in the building of $2A5NP^+$ cationic acentric packings. For instance, the dimensions of NO_3^- are too small to hinder dipole–dipole interactions between two $2A5NP^+$ neighbours resulting in a local centrosymmetrical arrangement. In contrast, a half-way situation occurs in the bis(2-amino-5-nitropyridinium) tetrachlorocuprate structure: the first $2A5NP^+$ site is more crowded and exhibits polar packing (Bagieu-Beucher, Masse & Tranqui, 1991) whereas the less crowded site shows local centric packing inducing a centrosymmetrical structure. The dimensions of $CuCl_4^{2-}$ are suitable for inducing a shielding effect, but a second cation site is needed to balance the charge, a situation which creates denser packing and consequently favours mutual dipolar interactions. The anionic shielding effect becomes efficient when polymeric monovalent anions like $(H_2PO_4^-)_n$, $(H_2AsO_4^-)_n$ *etc.* are used as host matrices. Our strategy, which uses anions to build polar packing of nitroaniline entities, may be compared to that employed in the organic molecular crystal engineering of 2-cyclooctylamino-5-nitropyridine (COANP) (Günter, Bosshard, Sutter, Arend, Chapuis, Twieg & Dobrowolski, 1987) and 2-adamantylamino-5-nitropyridine (AANP) (Nicoud, 1988; Tomaru, Matsumoto, Kurihara, Suzuki, Ooba & Kaino, 1991).

COANP and AANP are crystalline materials in which the bulky cyclooctyl and adamantyl groups induce polar ordering of 2-amino-5-nitropyridine entities like $(H_2PO_4^-)_n$ in 2A5NPDP (Fig. 6) or $Cr_2O_7^{2-}$ in bis(2-amino-5-nitropyridinium) dichromate. The same role is played by polymeric anionic subnetworks, large anions or bulky groups in ordering the 2-amino-5-nitropyridine entities in a 'herringbone' structure (the same $Pna2_1$ space group describes all these structures!). We can further envisage the design of 'cocrystals' containing 2A5NP molecules with the same 'herringbone' structure since relevant studies now support the design of organic 'cocrystals' where the packing of dipolar entities is ensured through a selective hydrogen-bond network (Etter, Urbanczyk-Lipkowska, Zia-Ebrahimi & Panunto, 1990; Gieb, Hirst, Vicent & Hamilton, 1991).

Compared to the traditional engineering route for obtaining non-linear optical organic crystals our approach has two main advantages:

(i) There is a shift towards the blue wavelength region of crystal transparency owing to the less polarizable nature of the 2-amino-5-nitropyridinium

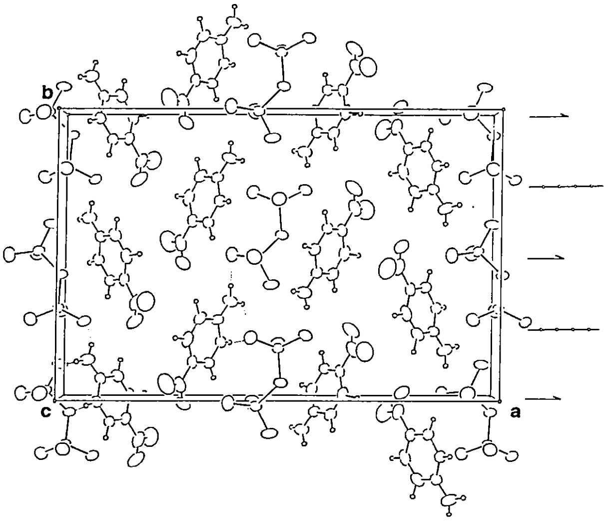

Fig. 3. *ORTEP* drawing of the structure of bis(2-amino-5-nitropyridinium) dichromate. Thermal ellipsoids are drawn at the 50% probability level for the non-hydrogen atoms.

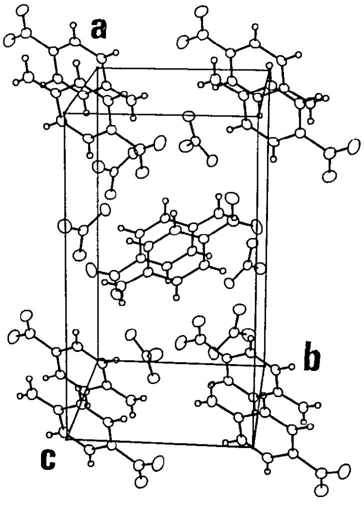

Fig. 4. Antiparallel arrangement of cations in 2-amino-5-nitropyridinium nitrate.

cation compared to molecular equivalent. $\lambda_{\text{cut-off}} =$ 420 nm has been observed in the 2A5NPDP crystal (Kotler, Hierle, Josse, Zyss & Masse, 1992).

(ii) Crystal growth is easier than that of molecular crystals: the non-linear optical cationic entities are strongly anchored onto the anionic inorganic frameworks through short hydrogen bonds giving the packing the cohesiveness observed in ionic inorganic crystals. The building of such crystals is less sensitive to stacking faults than molecular crystals.

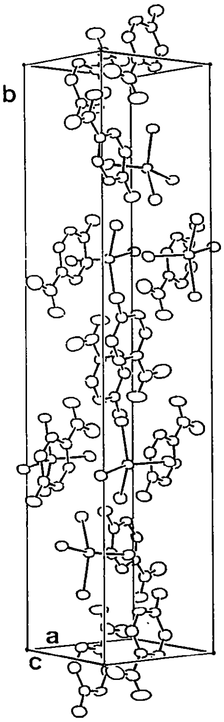

Fig. 5. Three-dimensional structure of bis(2-amino-5-nitropyridinium) tetrachlorocuprate. One site of $2A5NP^+$ is partly arranged in herringbone framework.

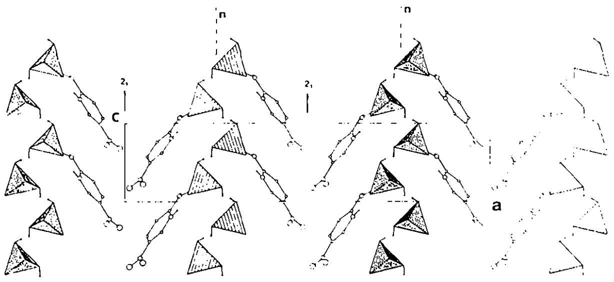

Fig. 6. *ac* projection of 2-amino-5-nitropyridinium dihydrogenmonophospate showing the herringbone framework of $2A5NP^+$ cations.

We thank Dr J. Zyss and Dr R. Hierle for their interest in this new non-linear optical crystal engineering route and for SHG powder tests performed at the Molecular Quantum Electronics Department, Bagneux, France-Télécom, France.

References

Bagieu-Beucher, M., Masse, R. & Tranqui, D. (1991). *Z. Anorg. Allg. Chem.* **606**, 59–71.

Bierlein, J. D. & Vanherzeele, H. (1989). *J. Opt. Soc. Am. B*, **6**, 622–633.

Bondi, A. (1964). *J. Phys. Chem.* **68**, 441–451.

Chen, C., Wu, B., Jiang, A. & You, G. (1984). *Sci. Sin.* **B27**, 598–604.

Chen, C., Wu, Y., Jiang, A., Wu, B., Li, R. & Lin, S. (1989). *J. Opt. Soc. Am. B*, **6**, 616–621.

Colapietro, M., Domenicano, A., Marciante, C. & Portalone, G. Z. (1982). *Z. Naturforsch. Teil B*, **37**, 1309–1311.

Dewar, M. (1950). *J. Chem. Soc.* pp. 2329–2334.

Enraf–Nonius (1977). *Structure Determination Package*. Enraf–Nonius, Delft, The Netherlands.

Etter, M. C., Urbanczyk-Lipkowska, Z., Zia-Ebrahimi, M. & Panunto, T. W. (1990). *J. Am. Chem. Soc.* **112**, 8415–8426.

Gieb, S. J., Hirst, S. C., Vicent, C. & Hamilton, A. D. (1991). *J. Chem. Soc. Chem. Commun.* pp. 1283–1285.

Guñter, P., Bosshard, C., Sutter, K., Arend, H., Chapuis, G., Twieg, R. J. & Dobrowolski, D. (1987). *Appl. Phys. Lett.* **50**, 486–488.

Johnson, C. K. (1965). *ORTEP*. Report ORNL-3794. Oak Ridge National Laboratory, Tennessee, USA.

Kotler, Z., Hierle, R., Josse, D., Zyss, J. & Masse, R. (1992). *J. Opt. Soc. Am. B*, **9**, 534–547.

Kurtz, S. K. & Perry, T. T. (1968). *J. Appl. Phys.* **39**, 3798–3813.

Lu, S.-F., Ho, M.-Y. & Huang, S.-L. (1982). *Acta Phys. Sin.* **31**, 948–955.

Main, P., Lessinger, L., Woolfson, M. M., Germain, G. & Declercq, J.-P. (1977). *MULTAN77. A System of Computer Programs for the Automatic Solution of Crystal Structures from X-ray Diffraction Data.* Univs. of York, England, and Louvain, Belgium.

Masse, R. & Zyss, J. (1991). *Mol. Eng.* **1**, 141–152.

Masse, R., Zyss, J., Bagieu-Beucher, M. & Levy, J. P. (1993). *Adv. Mater.* Submitted.

Meredith, G. R. (1983). *Nonlinear Optical Properties of Organic and Polymeric Materials*, ACS Symposium Series No. 233, pp. 27–56. Washington, DC: American Chemical Society.

Nicoud, J. F. (1988). *Mol. Cryst. Liq. Cryst.* **156**, 257–259.

Pecaut, J., Le Fur, Y. & Masse, R. (1993). *Acta Cryst.* **B49**. In the press.

Stout, G. H. & Jensen, L. H. (1968). *X-ray Structure Determination*, pp. 411–412. London: Macmillan.

Tam, W., Guerin, B., Calabrese, J. C. & Stevenson, S. M. (1989). *Chem. Phys. Lett.* **154**, 93–96.

Tomaru, S., Matsumoto, S., Kurihara, T., Suzuki, H., Ooba, N. & Kaino, T. (1991). *Appl. Phys. Lett.* **58**, 2583–2485.

Trueblood, K. N., Goldish, E. & Donohue, J. (1961). *Acta Cryst.* **14**, 1009–1017.

Zumsteg, F. C., Bierlein, J. D. & Gier, T. E. (1976). *J. Appl. Phys.* **47**, 4980–4985.

Zyss, J. (1990). *Conjugated Polymeric Materials: Opportunities in Electronics, Optoelectronics and Molecular Electronics*, edited by J. L. Bredas & R. R. Chance, pp. 545–557. Dordrecht: Kluwer Academic Publishers.

Zyss, J., Chemla, D. S. & Nicoud, J. F. (1981). *J. Chem. Phys.* **74**, 4800–4811.

Zyss, J., Nicoud, J. F. & Coquillay, M. (1984). *J. Chem. Phys.* **81**, 4160–4167.

Zyss, J. & Oudar, J. L. (1982). *Phys. Rev. A*, **26**, 2028–2048.